

Diffusion thermo effects on unsteady MHD free convection flow of a Kuvshinski fluid past a vertical porous plate in slip flow regime

Sivakumar Narsu and B Rushi Kumar

Department of Mathematics, School of Advanced Sciences, VIT University, Vellore-632014, India

E-mail: rushikumar@vit.ac.in

Abstract. The main purpose of this work is to investigate the diffusion-thermo effects on unsteady combined convection magneto-hydrromagnetic boundary layer flow of viscous electrically conducting and chemically reacting fluid over a vertical permeable radiated plate embedded in a highly porous medium. The slip flow regime is applied at the porous interface a uniform magnetic field is applied normal to the fluid flow direction which absorbs the fluid with suction that varies with time. The dimensionless governing equations are solved analytically using two terms harmonic and non-harmonic functions. The expressions for the fields of velocity, temperature and concentration are obtained. For engineering interest we also calculated the physical quantities the skin friction coefficient, Nusselt and Sherwood number are derived. The effects of various physical parameters on the flow quantities are studied through graphs and tables. For the validity, we have checked our results with previously published work and found good agreement with already existing studies.

Nomenclature.

x^* , y^* dimensional distances	Du Dufour number
t^* dimensional time	K_1 dimensional chemical reaction parameter
C_p specific heat at constant pressure	Sh Sherwood number
u^* , v^* dimensional velocity components	C_f Skin friction
C_s concentration susceptibility	Nu Nusselt number
T^* dimensional temperature	V_0 suction velocity
D_m molecular diffusivity	Greek Symbols
C^* dimensional concentration	μ coefficient of viscosity
D mass diffusivity	κ thermal conductivity



T_w temperature at the wall	ε constant
C_w dimensional concentration at the wall	ρ density
T_∞ dimensional temperature at free stream	σ electrical conductivity
A suction velocity parameter	λ coefficient of Kuvshinski fluid
C_∞ free stream dimensional concentration	κ thermal conductivity
Q_o coefficient of dimensional	ν kinematic viscosity
Q_1^* radiation absorption	β_T thermal expansion coefficient
K^* permeability of the porous medium	β_c concentration expansion coefficient
V_0 suction velocity	
h_1 refraction parameter	Superscripts
g acceleration due to gravity	* dimensional properties
Gr thermal Grashof number	' differentiation with respect to y
Gm concentration Grashof number	Subscripts
K_T thermal diffusion ratio	w, ∞ wall and free stream condition

1. Introduction

Convective flows with concurrent heat and mass transfer under the influence of a magnetic field, chemical reaction, and thermal radiation arise in many transport processes that has applications in many branches of science and engineering. This phenomenon plays a vital role in the chemical industry, chemical vapor deposition on surfaces, cooling of nuclear reactors, power and cooling industry for drying, and petroleum industries. Recently Anjalidevi and Kandasamy [1], Elbashbeshy [2], Shateyi and Motsa [3], Raju and Chamka et al. [4] are studied the Soret effect due to mixed convection on unsteady magnetohydrodynamic flow past a semi infinite vertical permeable moving plate in presence of thermal radiation, heat absorption and homogeneous chemical reaction. Ibrahim et al. [5] considered the effects of chemical reaction and radiation absorption on unsteady MHD free convection flow past a semi- infinite vertical permeable moving plate with heat source and suction. Vidya Sagar and Raju et al. [6] examined an unsteady magnetohydrodynamic (MHD) radiation absorption free convective boundary layer flow of Kuvshinski fluid in the presence of a porous medium.

At the macroscopic level, it is well known that the boundary condition due to viscous fluid at the solid wall is one of the no slip is said the fluid velocity of the solid boundary. While the no-slip condition has been treated experimentally to be accurate for a number of macroscopic flows, it remains an assumption that is not based on physical principles. The particle at the surface has a finite tangential velocity. In engineering applications, the study of magneto-micropolar fluid flows in the slip flow regimes with heat transfer, for example, the power generators, refrigeration coils, electric transformers, transmission lines, and heating elements. Khandelwal et al. [7] proposed the effects of permeability variation on the Magnetohydrodynamic (MHD) an unsteady flow of micropolar fluid through a porous medium in a slip flow regime over an infinite porous flat plate. Sharma and Chaudhary [8] analyzed free convective heat and mass transfer effect of variable suction on viscous incompressible fluid flows past a vertical porous plate in a slip flow regime. Recently, Sharma [9] demonstrated the effects of periodic temperature and concentration on unsteady free stream consisting of a mean velocity over an

exponentially varying with time. Chaudhary and Jha [10] discussed the numerical study of chemically reactive MHD micropolar fluid flow past a vertical plate in slip flow regime.

Jyothi et al. [11] presently chemical and thermo-diffusion effects on MHD free convection flow through a porous medium in a slip flow regime. Effects on the magnetohydrodynamic free convective vertical porous plate due to diffusion-thermo and thermo-diffusion embedded in a non-Darcian porous medium have been examined by Ramachandra Prasad et al. [12]. Heat and mass transfer free convective MHD flow of a porous diffusion-thermo over an inclined surface has been demonstrated by Durga Prasad et al. [13]. Krishna Reddy et al. [14] studied heat and mass transfer MHD flow of Kuvshinski fluid with temperature gradient dependent heat source effects over a vertical porous surface in the presence of variable heat and mass flux. Varma et al. [15] developed an analysis of magnetohydrodynamic heat and mass transfer micropolar fluid with convective diffusion-thermo effects. Sekhar et al. [16] investigated the effects of heat and mass transfer MHD free convective diffusion-thermo and radiation absorption with a porous plate in a slip flow regime. Slip effects of viscous dissipation on unsteady MHD flow over a stretching sheet studied by Sekhar and Viswanatha Reddy [17].

As per the author's knowledge, the interaction between the chemical reaction and diffusion-thermo in the presence of radiation absorption, porous medium effects has received little attention. Hence, an attempt is made to study the diffusion-thermo effects on an unsteady heat and mass transfer MHD free convection flow of a viscous incompressible electrically conducting Kuvshinski fluid through a porous medium from a vertical porous plate with varying suction velocity in slip flow regime.

2. Mathematical formulation

A two dimensional unsteady magnetohydrodynamic (MHD) flow past a vertical infinite plate embedded in a porous medium has been considered with the viscoelastic fluid model. A uniform transverse magnetic field B_0 is applied normal to the direction of the fluid flow direction, let x^* -axis taken along the flow in the vertical direction and y^* -axis is taken perpendicular to it. The presence of chemical reaction, Dufour effect, and a heat source or sink parameters are also considered along with buoyancy effects past a vertical porous plate with a dependent heat source in slip flow regime with uniform velocity u_p^* . The physical model of the problem as shown in Figure 1.

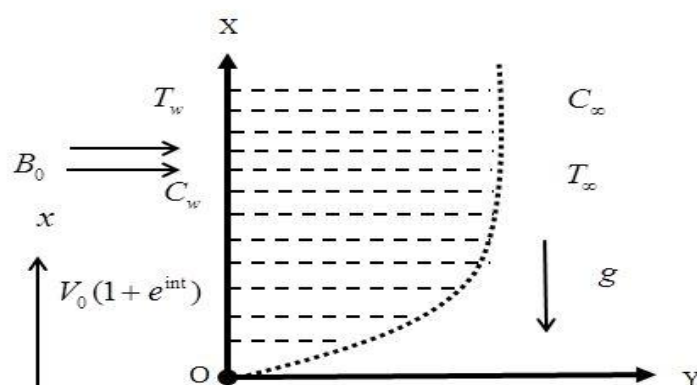


Figure 1. Physical Model

In the analysis, the following assumptions are made

1. The flow is unsteady and laminar.
2. The plate is taken that sufficiently long enough is very small, so the all the physical quantities are taken as the functions of y and t only.
3. The induced magnetic field is neglected because magnetic Reynolds number is very small.
4. The effects of Viscous and Joule's dissipation are neglected.
5. Now assumed that all the fluid flow properties to be constant except that of the impact of density variation temperature.

$$\frac{\partial v^*}{\partial y^*} = 0 \quad (1)$$

$$\left(1 + \lambda \frac{\partial}{\partial t^*}\right) \frac{\partial u^*}{\partial t^*} + v^* \frac{\partial u^*}{\partial y^*} = \nu \frac{\partial^2 u^*}{\partial y^{*2}} + g\beta_T (T^* - T_\infty) + g\beta_C (C^* - C_\infty) - \left(\frac{\sigma B_0^2}{\rho} + \frac{\nu}{K^*}\right) \left(1 + \lambda \frac{\partial}{\partial t^*}\right) u^* \quad (2)$$

$$\left(1 + \lambda \frac{\partial}{\partial t^*}\right) \frac{\partial T^*}{\partial t^*} + v^* \frac{\partial T^*}{\partial y^*} = \frac{k}{\rho C_p} \frac{\partial^2 T^*}{\partial y^{*2}} - \frac{Q_0}{\rho C_p} (T^* - T_\infty) + Q_1^* (C^* - C_\infty) + \frac{D_m K_T}{C_s \rho C_p} \frac{\partial^2 C^*}{\partial y^{*2}} \quad (3)$$

$$\left(1 + \lambda \frac{\partial}{\partial t^*}\right) \frac{\partial C^*}{\partial t^*} + v^* \frac{\partial C^*}{\partial y^*} = D \frac{\partial^2 C^*}{\partial y^{*2}} - K_1 (C^* - C_\infty) \quad (4)$$

The appropriate boundary conditions are for the velocity, temperature and species diffusion fields are

$$\begin{aligned} u^* &= u_p^* + L_1 \frac{du^*}{dy^*}, T^* = T_w + \varepsilon (T_w - T_\infty) e^{n^* t^*} \\ C^* &= C_w + \varepsilon (C_w - C_\infty) e^{n^* t^*} \text{ at } y^* = 0 \\ u^* &= 0, T^* \rightarrow T_\infty, C^* \rightarrow C_\infty \text{ at } y^* \rightarrow \infty \end{aligned} \quad (5)$$

Where n^* is constant velocity of the wall.

From Eq. (1) it is clear that the suction velocity at the plate is a function of time t only. Let us assume that

$$v^* = -V_0 \left(1 + \varepsilon A e^{n^* t^*}\right) \quad (6)$$

Where V_0 is the suction velocity and $\varepsilon A \ll 1$. The negative sign indicated that the suction velocity directed towards the plate.

By introducing the non-dimensional quantities are

$$\begin{aligned}
u &= \frac{u^*}{V_0}, v = \frac{v^*}{V_0}, y = \frac{V_0 y^*}{\nu}, t = \frac{V_0^2 t^*}{\nu}, u_p = \frac{u_p^*}{V_0}, n = \frac{n^* \nu}{V_0^2}, \theta = \frac{T^* - T_\infty}{T_w - T_\infty}, C = \frac{C^* - C_\infty}{C_w - C_\infty}, \\
Gr &= \frac{\nu g \beta_T (T_w - T_\infty)}{V_0^3}, Gm = \frac{\nu g \beta_c (C_w - C_\infty)}{V_0^3}, M = \frac{\sigma B_0^2 \nu}{\rho V_0^2}, K = \frac{K^* V_0^2}{\nu^2}, \gamma = \frac{K_1 \nu}{V_0^2}, \\
Q_1 &= \frac{\nu Q_1^* (C_w - C_\infty)}{(T_w - T_\infty) V_0^2}, \alpha_2 = \frac{\lambda V_0^2}{\nu}, Du = \frac{Dm K_T (C_w - C_\infty)}{C_s K (T_w - T_\infty)}, h_1 = \frac{L_1 V_0}{\nu}, \nu = \frac{\mu}{\rho}, Pr = \frac{\mu C_p}{\kappa}, \\
Sc &= \frac{\nu}{D}, \phi = \frac{Q_0 \nu}{\rho C_p V_0^2}
\end{aligned} \tag{7}$$

By using the above non-dimensional quantities, the Eqs. (2)-(4) can be expressed in a dimensionless form as

$$\frac{\partial u}{\partial t} + \alpha_2 \frac{\partial^2 u}{\partial t^2} - (1 + \varepsilon A e^{nt}) \frac{\partial u}{\partial y} = \frac{\partial^2 u}{\partial y^2} + Gr\theta + GmC - \left(M + \frac{1}{K}\right)u - \alpha_2 \left(M + \frac{1}{K}\right) \frac{\partial u}{\partial t} \tag{8}$$

$$\frac{\partial \theta}{\partial t} + \alpha_2 \frac{\partial^2 \theta}{\partial t^2} - (1 + \varepsilon A e^{nt}) \frac{\partial \theta}{\partial y} = \frac{1}{Pr} \frac{\partial^2 \theta}{\partial y^2} - \phi\theta + Q_1 C + Du \frac{\partial^2 C}{\partial y^2} \tag{9}$$

$$\frac{\partial C}{\partial t} + \alpha_2 \frac{\partial^2 C}{\partial t^2} - (1 + \varepsilon A e^{nt}) \frac{\partial C}{\partial y} = \frac{1}{Sc} \frac{\partial^2 C}{\partial y^2} - \gamma C \tag{10}$$

The corresponding initial and boundary conditions in Eq. (5) in a non-dimensional form are given below:

$$u = u_p + h_1 \frac{du}{dy}, \theta = 1 + \varepsilon e^{nt}, C = 1 + \varepsilon e^{nt} \text{ at } y = 0 \tag{11}$$

$$u \rightarrow 0, \theta \rightarrow 0, C \rightarrow 0 \text{ as } y \rightarrow \infty$$

3. Solution of the problem

The Eqs. (8)-(10) are coupled and non linear partial differential equations (PDEs) whose solutions in closed form are difficult to obtain, to solve these coupled non-linear partial differential equations, we assume that the unsteady flow, so that in the neighborhood of the plate, we have

$$\begin{aligned}
u(y, t) &= u_0(y) + \varepsilon e^{nt} u_1(y) + O(\varepsilon^2) \\
\theta(y, t) &= \theta_0(y) + \varepsilon e^{nt} \theta_1(y) + O(\varepsilon^2) \\
C(y, t) &= C_0(y) + \varepsilon e^{nt} C_1(y) + O(\varepsilon^2)
\end{aligned} \tag{12}$$

By substituting the Eq.(12) into the Eq.(8)-(10) the equations are reduced to harmonic and non-harmonic terms and neglecting the higher order terms in ε , we obtain

$$u_0'' + u_0' - \left(M + \frac{1}{K}\right)u_0 = -(Gr\theta_0 + GmC_0) \tag{13}$$

$$u_1'' + u_1' - \left(n + \alpha_2 n^2 + \left(M + \frac{1}{K}\right)(1 + \alpha_2 n)\right)u_1 = -(Gr\theta_1 + GmC_1 + Au_0') \tag{14}$$

$$\theta_0'' + Pr\theta_0' - Pr\phi\theta_0 = -(PrQ_1C_0 + PrDuC_0'') \tag{15}$$

$$\theta_1'' + \text{Pr} \theta_1' - \text{Pr}(\phi + n + \alpha_2 n^2) \theta_1 = \text{Pr} Q_1 C_1 - \text{Pr} Du C_0'' - A \text{Pr} \theta_0' \quad (16)$$

$$C_0'' + \text{Sc} C_0' - \text{Sc} \gamma C_0 = 0 \quad (17)$$

$$C_1'' + \text{Sc} C_1' - \text{Sc}(\gamma + n + \alpha_2 n^2) C_1 = -A \text{Sc} C_0' \quad (18)$$

Now, the corresponding boundary conditions are:

$$u_0 = u_p + h_1 \frac{du_0}{dy}, u_1 = h_1 \frac{du_1}{dy}, \theta_0 = 1, \theta_1 = 1, C_0 = 1, C_1 = 1 \text{ at } y = 0$$

$$u_0 \rightarrow 0, u_1 \rightarrow 0, \theta_0 \rightarrow 0, \theta_1 \rightarrow 0, C_0 \rightarrow 0, C_1 \rightarrow 0 \text{ as } y \rightarrow \infty \quad (19)$$

$$u(y, t) = (B_{11} e^{-m_9 y} + B_9 e^{-m_1 y} + B_{10} e^{-m_5 y}) + \varepsilon e^{nt} (B_{18} e^{-m_{11} y} + B_{13} e^{-m_1 y} + B_{14} e^{-m_3 y} + B_{15} e^{-m_5 y} + B_{16} e^{-m_7 y} + B_{17} e^{-m_9 y}) \quad (20)$$

$$\theta(y, t) = ((1 - B_3) e^{-m_5 y} + B_3 e^{-m_1 y}) + \varepsilon e^{nt} (B_8 e^{-m_7 y} + B_5 e^{-m_1 y} + B_6 e^{-m_3 y} + B_7 e^{-m_5 y}) \quad (21)$$

$$C(y, t) = e^{-m_1 y} + \varepsilon e^{nt} (1 - B_2) e^{-m_3 y} + B_2 e^{-m_1 y} \quad (22)$$

For engineering purpose, the friction factor, local Nusselt number and local Sherwood number are given by

$$\tau_w = \mu \frac{\partial u^*}{\partial y^*} \text{ at } y^* = 0$$

Where $\tau_w = \rho V_0^2 u'(0)$

$$C_f = (-m_9 B_{11} - m_1 B_9 - m_5 B_{10}) + \varepsilon e^{nt} (-m_{11} B_{18} - m_1 B_{13} - m_3 B_{14} - m_5 B_{15} - m_7 B_{16} - m_9 B_{17}) \quad (23)$$

$$Nu_x = \frac{q_w}{T_w - T_\infty} \frac{x}{k}$$

$$\frac{Nu}{\text{Re}_x} = -\theta_0' = ((1 - B_3) m_5 + m_1 B_3) + \varepsilon e^{nt} (m_7 B_8 + m_1 B_5 + m_3 B_6 + m_5 B_7) \quad (24)$$

Where $\text{Re}_x = \frac{V_0 x}{\nu}$

$$Sh = x \left(\frac{\partial c / \partial y^*}{C_w - C_\infty} \right) \text{ at } y^* = 0$$

$$\begin{aligned} \frac{Sh}{\text{Re}_x} &= \frac{\partial c}{\partial y} \text{ at } y = 0 \\ &= -m_1 + \varepsilon e^{nt} (-m_3)(1 - B_2) - m_1 B_2 \end{aligned} \quad (25)$$

4. Results and Discussion

The analytical solutions are transformed for velocity, temperature and concentration profiles for different values of physical parameters as Magnetic field parameter M , Dufour number Du , thermal Grashof number Gr , mass Grashof number Gm , Schmidt number Sc , radiation absorption parameter Q_1 , porosity parameter K , chemical reaction parameter γ , Visco-elastic parameter α_2 , Prandtl number Pr , and heat source parameter ϕ are depicted from figures 1-18. We assign values to the parameters as $n = 1, A = 1; Sc = 0.22, t = 1, U_p = 1.5, \varepsilon = 0.02, Pr = 0.71, Gr = 5, Gm = 5$.

The effect of magnetic field on velocity profile is plotted in Figure. 5. It is clear that the increasing values of magnetic field parameter decrease the velocity profiles. This validates the general behavior of magnetic field. Physically, the rising values of magnetic field generate opposing force to the flow direction, this force is called Lorentz force. Due to this cause, we have seen a decrement in the velocity field.

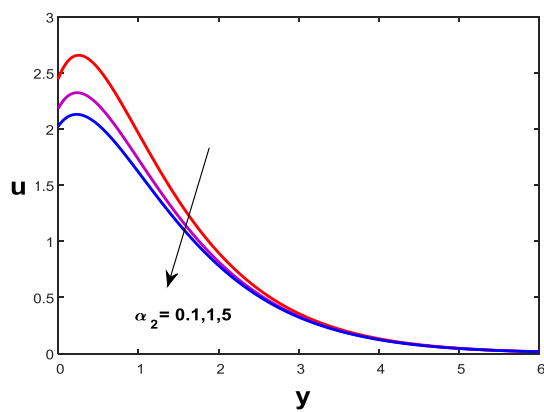


Figure 2. Effects of α_2 on Velocity profiles

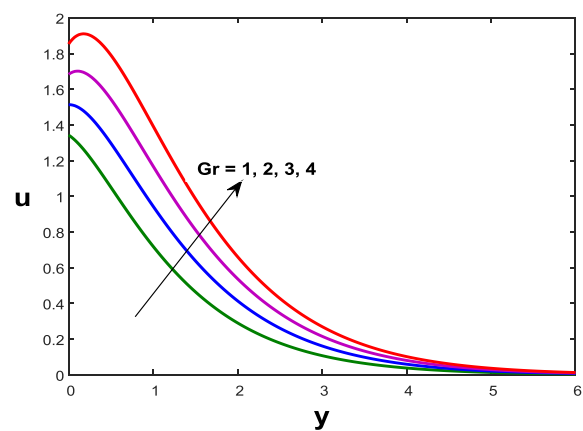


Figure 3. Effects of Gr on Velocity profiles

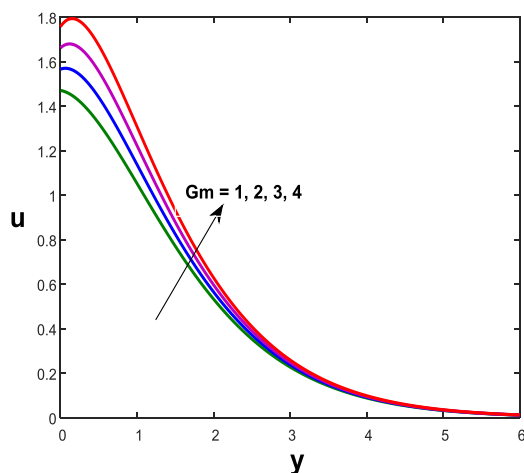


Figure 4. Effects of Gm on Velocity profiles

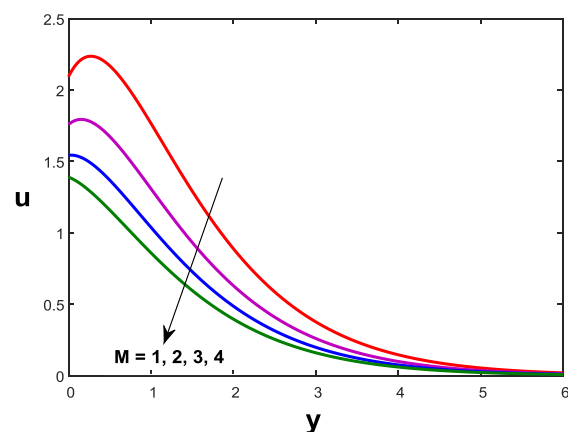


Figure 5. Effects of M on Velocity profiles

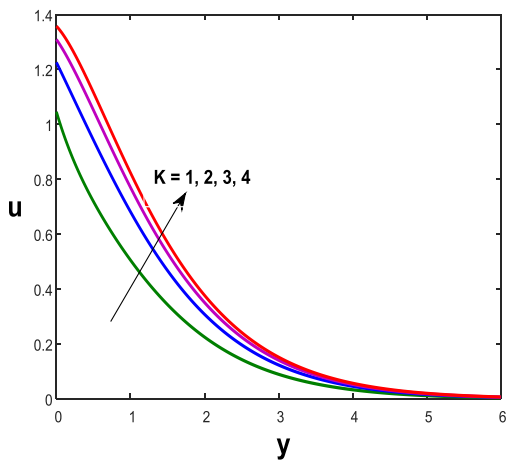


Figure 6 Effects of K on Velocity profiles

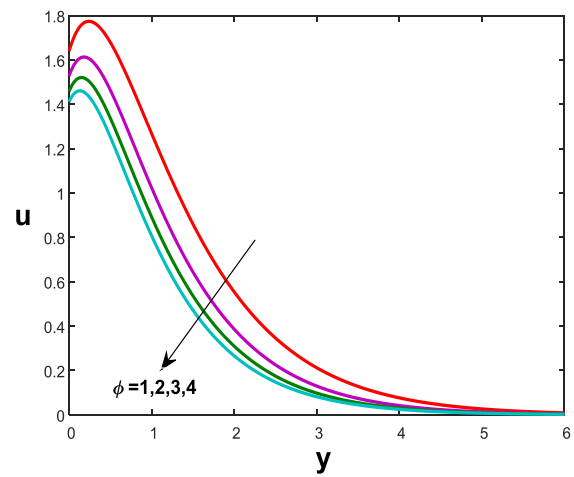


Figure 7. Effects of ϕ on Velocity profiles

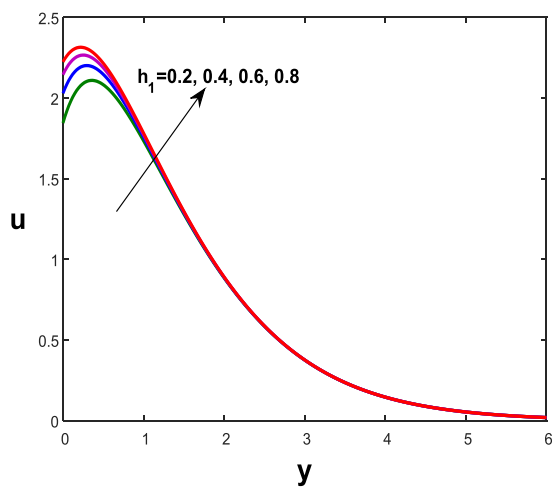


Figure 8. Effects of h_1 on Velocity profiles

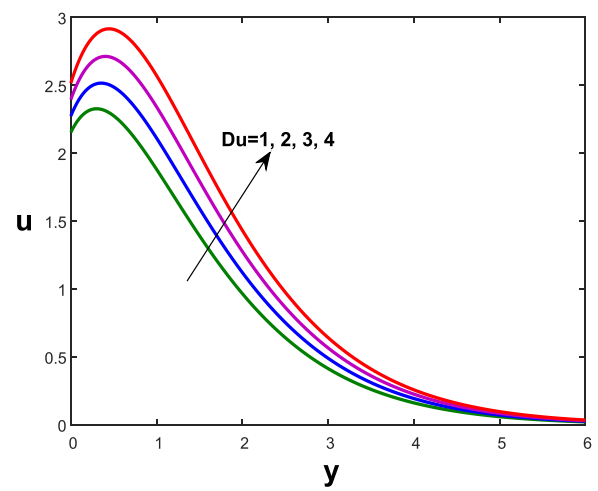


Figure 9. Effects of Du on Velocity profiles

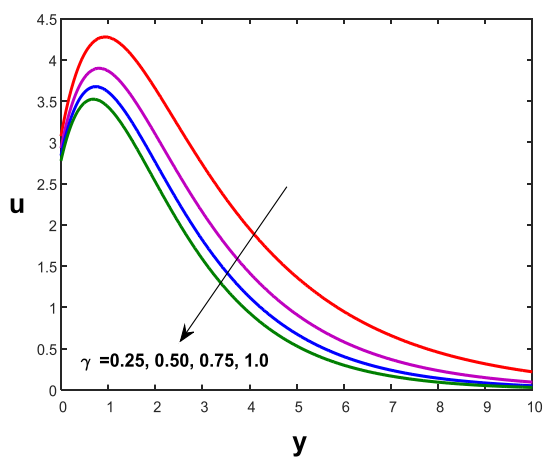


Figure 10. Effects of γ on Velocity profiles

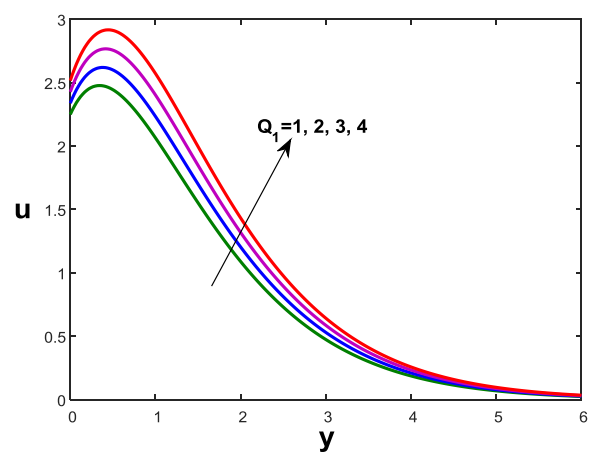


Figure 11. Effects of Q_1 on Velocity profiles

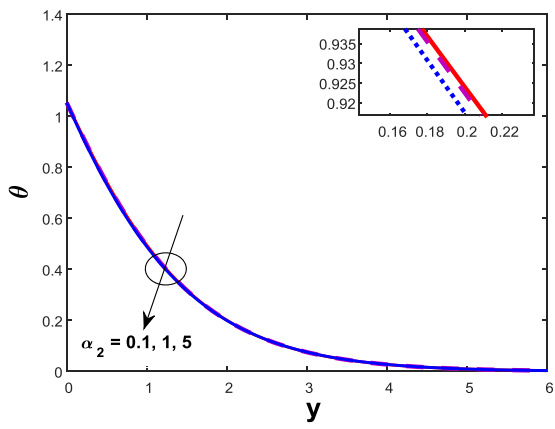


Figure 12. Effects of α_2 on Temperature profiles

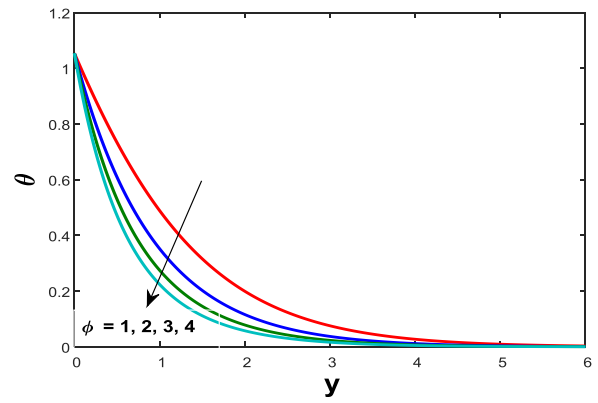


Figure 13. Effects of ϕ on Temperature profiles

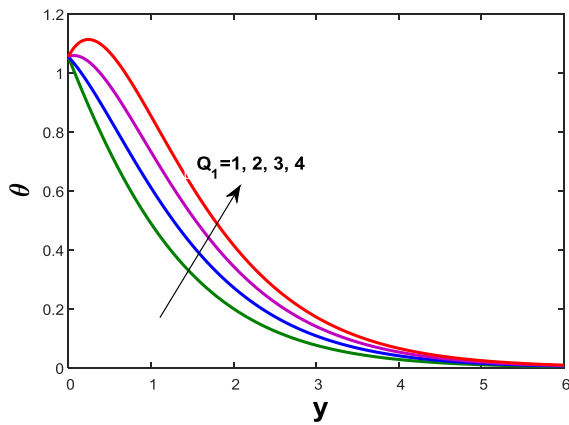


Figure 14. Effects of Q_1 on Temperature profiles

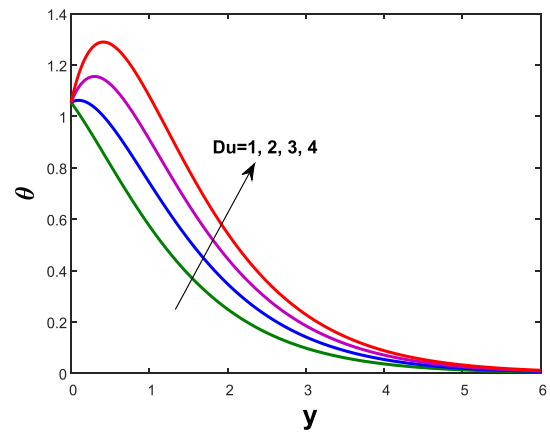


Figure 15. Effects of Du on Temperature profiles

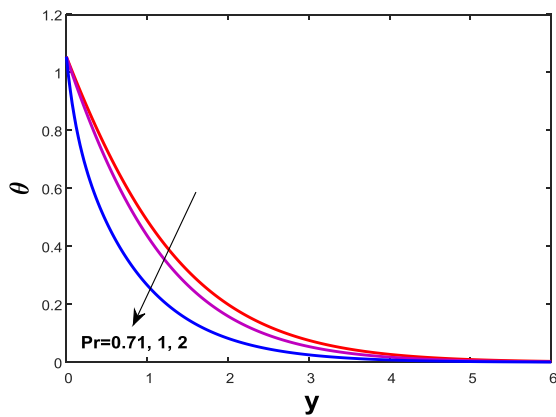


Figure 16. Effects of Pr on Temperature profiles

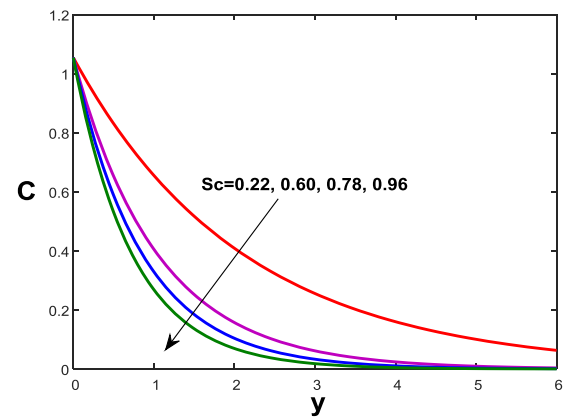


Figure 17. Effects of Sc on Concentration profiles

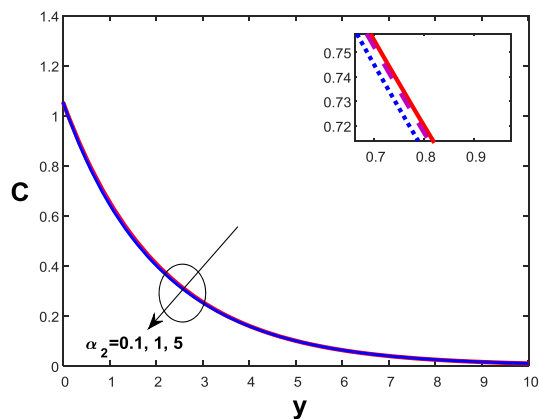


Figure 18. Effects of α_2 on Concentration profiles

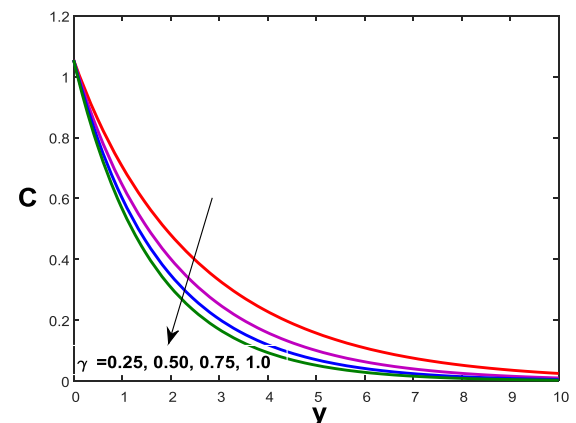


Figure 19. Effects of γ on Concentration profiles

Figures 3 and 4 show the effect of thermal and concentration buoyancy forces on velocity field. It is noted from that the increasing values of Gr and Gm improves the velocity field. Generally, raising the values of Gr and Gm keeps more pressure on the flow due to this we saw an increment in velocity field.

The porosity parameter on velocity distributions is depicted in Figure. 6. It is observed that the enhancing value of porosity parameter increases the velocity distributions. The improving values of K increases the permeability; this can lead to improving the velocity profiles.

Figures 2, 12 and 18 show the effect of α_2 on velocity, temperature and concentration profiles. It is observed that the increasing values of α_2 decreases the velocity, temperature, and concentration fields. This may happen due to the domination of viscous nature in the flow. The similar behavior was observed in the presence of Prandtl number it is shown in Figures. 16. The effect of ϕ on velocity and temperature fields is shown in Figures 7 and 13. It is observed that the heat source parameter depreciates the velocity and temperature fields.

The quite similar behavior was observed in Figures. 17. It shows the effect of Schmidt number on concentration field. From Figures 11 and 14 show the increase in velocity and temperature profiles with increasing values of Q_1 . The effect of refraction parameter h_1 on velocity profiles is shown in Figure. 8. This validates the general behavior of slip. Basically, increasing values of slip parameter improve the thickness of the boundary layer this can help to enhance the velocity profiles. Figures 10 and 19 show the effect of chemical reaction parameter on velocity and concentration profiles. It is clear that the increasing the values of chemical reaction parameter depreciate the velocity and concentration profiles. The effect of Dufour number Du on velocity and temperature profiles is plotted in Figures 9 and 15. It is observed that the increasing values of Du increases the velocity as well as temperature profiles, due to the domination of interfacial mass transfer in the flow.

Table 1. The variations in Skin friction, Nusselt and Sherwood number for various values of

$$A = 1, Gr = 5, Gm = 20, Pr = 0.71$$

Sc	α_2	Q_1	ϕ	M	K	γ	Harinath Reddy et al. [18]			Present Work ($Du = 0, h_1 = 0$)		
							Cf	Nu	Sh	Cf	Nu	Sh
0.22	1	1	1	1	1	1	14.2065	-0.6478	-0.7008	14.2046	-0.9569	-0.7078
0.60	1	1	1	1	1	1	9.4799	-1.2384	-0.7267	10.7843	-1.2384	-0.7267
0.78	1	1	1	1	1	1	9.5134	-1.4851	-0.7600	9.3692	-1.4861	-0.7607
0.96	1	1	1	1	1	1	8.6703	-1.7218	-0.7008	8.6088	-1.7318	-0.7108
0.22	2	1	1	1	1	1	13.2966	-0.6541	-0.7472	13.2866	-0.6561	-0.7452
0.22	3	1	1	1	1	1	13.2425	-0.6597	-0.7593	13.3425	-0.6697	-0.7892
0.22	1	2	1	1	1	1	12.5446	-1.2443	3.7735	12.6543	-1.2443	3.7735

0.22	1	3	1	1	1	1	13.8542	-1.2443	6.3093	13.8542	-1.2443	6.3093
0.22	1	4	1	1	1	1	15.1638	-1.2443	8.8451	15.638	-1.2443	8.8451
0.22	1	1	2	1	1	1	10.2886	-1.2443	-0.3650	10.2886	-1.2443	-0.4650
0.22	1	1	3	1	1	1	9.6995	-1.2443	-1.6204	9.6985	-1.2443	-1.6294
0.22	1	1	4	1	1	1	9.5256	-1.2443	-1.8933	9.5256	-1.2443	-1.8833
0.22	1	1	1	2	1	1	9.2178	-1.2443	1.2377	9.2178	-1.2443	1.2377
0.22	1	1	1	3	1	1	7.8009	-1.2443	1.2377	7.8009	-1.2443	1.2377
0.22	1	1	1	4	1	1	6.7174	-1.2443	1.2377	6.7175	-1.2443	1.2377
0.22	1	1	1	1	2	1	12.6597	-1.2443	1.2377	12.6597	-1.2443	1.2377
0.22	1	1	1	1	3	1	13.2362	-1.2443	1.2377	13.2354	-1.2443	1.2377
0.22	1	1	1	1	4	1	13.5496	-1.2443	1.2377	13.5496	-1.2443	1.2377
0.22	1	1	1	1	1	5	11.2350	-1.2443	1.2377	11.3350	-1.2443	1.2377
0.22	1	1	1	1	1	10	8.6426	-1.6980	-0.9057	8.6926	-1.7980	-0.9057
0.22	1	1	1	1	1	15	7.6589	-2.0473	-0.9780	7.6789	-2.9473	-0.9780
0.22	1	1	1	1	1	20	6.9966	-2.3424	-1.0163	6.9866	-2.3524	-1.5163

5. Comparison of the results

In order to explain the accuracy of the present results of the study, it is considered that the analytical solutions obtained are compared with the numerical results for friction coefficient, local Nusselt and Sherwood numbers respectively. These calculated and compared results are presented in Table 1. From this Table 1, it is interesting to watch that the present results in the absence of diffusion-thermo and refraction parameters (h_1) are in good agreement with the corresponding results obtained from Harinath Reddy et al. [18].

6. Conclusion

The velocity of the plate for the Kuvshinski fluid which is exposed to a transverse magnetic field can be maintained constantly, the obtained partial differential equations (PDEs) are expressed in the dimensional form using non-dimensional quantities. These equations are solved analytically by using perturbation technique through graphs are obtained by to study the effects of different physical

parameters on temperature, velocity, and species diffusion profiles. In the current study, the following conclusions can be drawn:

1. Velocity decreases for an increase in Visco-elastic parameter α_2 , the radiation parameter Q_1 , the Schmidt number Sc , the permeability parameter K , the magnetic field parameter M , chemical reaction parameter γ and increases for an increase in mass Grashof number Gm .
2. Temperature profiles increased for an increase in α_2 , decreased due to in heat absorption coefficient ϕ , radiation parameter Q_1 and chemical reaction parameter as well as Schmidt number Sc .
3. Velocity and temperature distributions are increased for an increase in diffusion-thermo effect Du .

Appendix

$$\begin{aligned}
 m_1 &= \frac{Sc + \sqrt{Sc^2 + 4Sc\gamma}}{2} & m_3 &= \frac{Sc + \sqrt{Sc^2 + 4ScB_1}}{2} & m_5 &= \frac{Pr + \sqrt{Pr^2 + 4Pr\phi}}{2} \\
 m_7 &= \frac{Pr + \sqrt{Pr^2 + 4PrB_4}}{2} & m_9 &= \frac{1 + \sqrt{1 + 4M_1}}{2} & m_{11} &= \frac{1 + \sqrt{1 + 4B_{12}}}{2} \\
 B_1 &= \gamma + n + \alpha_2 n^2 & B_2 &= \frac{AScm_1}{m_1^2 - Scm_1 - ScB_1} & B_3 &= \frac{-(PrQ_1 + PrDum_1^2)}{m_1^2 - Prm_1 - Pr\phi} \\
 B_4 &= \phi + n + \alpha_2 n^2 & B_5 &= \frac{APr m_1 B_3 + Pr Q_1 B_2 - Pr Du B_2 m_1^2}{m_1^2 - Pr m_1 - Pr B_4} \\
 B_6 &= \frac{(PrQ_1 - PrDum_3^2)(1 - B_2)}{m_3^2 - Prm_3 - PrB_4} \\
 B_7 &= \frac{APr m_5 (1 - B_3)}{m_5^2 - Prm_5 - PrB_4} & B_8 &= 1 - (B_5 + B_6 + B_7) & B_9 &= \frac{-(GrB_3 + Gm)}{m_1^2 - m_1 - M_1} \\
 B_{10} &= \frac{-Gr(1 - B_3)}{m_5^2 - m_5 - M_1} & B_{11} &= \frac{u_p - B_9 - B_{10} - B_9 h_1 m_1 - B_{10} h_1 m_5}{1 + h_1 m_9} \\
 B_{12} &= n + \alpha_2 n^2 + M_1 (1 + \alpha_2 n) & B_{13} &= \frac{AB_9 m_1 - GrB_5 - GmB_2}{m_1^2 - m_1 - B_{12}} \\
 B_{14} &= \frac{-GrB_6 - Gm(1 - B_2)}{m_3^2 - m_3 - B_{12}} & B_{15} &= \frac{AB_{10} m_5 - GrB_7}{m_5^2 - m_5 - B_{12}}.
 \end{aligned}$$

Acknowledgement:

We are very much thankful to anonymous reviewers for their valuable comments and suggestions to improve this manuscript.

References

- [1] Anjalidevi SP, Kandasamy R 2000 *J. Appl. Math. Mech.* **80** 697–701
- [2] Elbashbeshy EMA 2003 *Appl. Math. Comput.* **136** 139–149

- [3] Shateyi S, Motsa SS 2010 *Adv. Top. Mass Trans.* 145–162
- [4] Raju MC, Chamka A J, Philip J, Varma SVK, *Int. J. Appl. Comput. Math.*
- [5] Ibrahim FS, Elaiw AM, Bakar AA 2008 *Communications in Non-Linear Science and Numerical Simulation* **13** 1056-1066
- [6] Vidya Sagar B, Raju MC, Varma SVK, Venkataramana S 2013, *Review of Adv. in Phy. Theories and Applications* **1** 48-62
- [7] Khandelwal K, Anil Gupta, Poonam, Jain N C Ganita 2003 **54**(2) 203–212
- [8] Sharma P K, Chaudhary R C Emirates 2008 *J. of Engg. Research*, **8**(2) 33-38
- [9] Sharma P K J. Matematicas 2005 XIII(1) 51-62
- [10] Chaudhary R C, Abhay Kumar Jha 2008 *Appl. Math. Mech. Engl. Ed.*, **29**(9) 1179-1194
- [11] Jyothi P, Viswanatha Reddy G, VijayakumarVarma S 2013 *Int. J. of Adv. Eng. Tech.* 33-36
- [12] Ramachandra Prasad V, Vasua B, Anwar O 2013 *Chemical Engineering Journal* **17** 598-606
- [13] Durga Prasad P, Kiran Kumar RVMSS, Mamatha B, Varma SVK 2016 *Global Journal of Pure and Applied Mathematics*.**12**(1) 142-150
- [14] Krishna Reddy V, Viswantha Reddy G, Kiran Kumar RVMSS, Durga Prasad P, Varma SVK 2016 *East Journal of Scientific Research* **24** (3) 593-602
- [15] Kiran Kumar RVMSS, Raju VCC, Durga Prasad P and Varma SVK *Applications And Applied Mathematics*, **11** 704 -721
- [16] Sekhar KR, Reddy GV, Varma SVK 2015 *Int. J. of Sci. and Inno. Math.Research* **3**(3) 1057-1061
- [17] Sekhar KR, Viswanatha Reddy G 2017 *i-manager's journal on mathematics*, **6**(1) 27-34
- [18] Harinath Reddy S, Raju MC, Keshava Reddy E 2017 *Int. J. Eng. Res. in Africa* **14** 13-27